Inorganic Chemistry

Article

pubs.acs.org/IC

Photochemical Redox Reactions of Copper(II)−Alanine Complexes in Aqueous Solutions

Chen-Jui Lin, Chao-Sheng Hsu, Po-Yen Wang, Yi-Liang Lin, Yu-Shiu Lo, and Chien-Hou Wu*

Department of Biomedical Engineering and Environmental Sciences, College of Nuclear Science, National Tsing Hua University, Hsinchu 30013, Taiwan

Supporting Information

ABSTRACT: The photochemical redox reactions of Cu(II)/alanine complexes have been studied in deaerated solutions over an extensive range of pH, Cu(II) concentration, and alanine concentration. Under irradiation, the ligand-to-metal charge transfer results in the reduction of Cu(II) to Cu(I) and the concomitant oxidation of alanine, which produces ammonia and acetaldehyde. Molar absorptivities and quantum yields of photoproducts for Cu(II)/alanine complexes at 313 nm are characterized mainly with the equilibrium Cu(II) speciation where the presence of simultaneously existing Cu(II) species is taken into account. By applying regression analysis, individual Cu(I) quantum yields are determined to be 0.094 ± 0.014 for the 1:1 complex (CuL) and 0.064 ± 0.012 for the 1:2 complex (CuL_2). Individual quantum yields of ammonia are 0.055 ± 0.007 for CuL and 0.036 ± 0.005 for CuL_2. Individual quantum yields of acetaldehyde are 0.030 ± 0.007 for CuL and 0.024 ± 0.007 for CuL_2. CuL always has larger quantum yields than CuL_2, which can be attributed to the Cu(II) stabilizing effect of the second ligand. For both CuL and CuL_2, the individual quantum yields of Cu(I), ammonia, and acetaldehyde are in the ratio of 1.8:1:0.7. A reaction mechanism for the formation of the observed photoproducts is proposed.

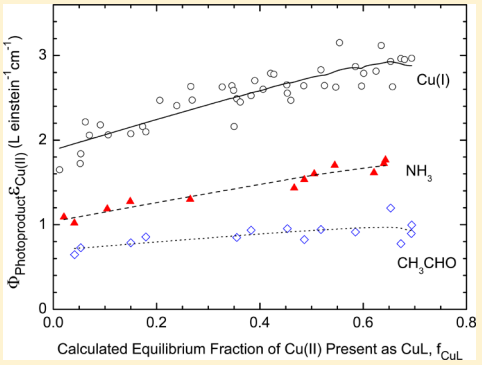

INTRODUCTION

There has been growing interest in the photochemical reactions of copper complexes in the environment and in biochemistry.[1−8] Copper is a ubiquitous transition metal, which has two accessible oxidation states. In natural waters and wastewaters, Cu(II) is thought to be present primarily as complexes with biogenic or anthropogenic ligands, many of which contain carboxylato and amino functional groups.[9−12] Copper complexes can participate in a large number of photochemical redox reactions in sunlit surface waters. The sunlight-initiated photoreactions of Cu(II) complexes may have significant effects on the speciation and geochemical cycling of copper, which, in turn, can affect the bioavailability or toxicity of copper in the upper water column.[13−16] The photoreactions of Cu(II) complexes are also accompanied by degradation of organic ligands or pollutants, which can contribute to the pollution abatement.[3] Photooxidation of Cu(II) complexes with pollutants, such as EDTA, NTA, and IDA, widely used in the detergent industry has been extensively studied in homogeneous and heterogeneous systems.[2,17−20] In the area of medicinal chemistry, copper complexes with various drugs may exhibit better biological activity in comparison to the drugs themselves.[21] The photoredox reactions of copper complexes can be used acting as redox scavengers for radicals photogenerated from drugs and biomolecules in antitoxic protective processes.[6,22,23] Several photolabile copper cages have been prepared and evaluated to induce oxidative stress as a cancer chemotherapy strategy.[24,25] Therefore, the photochemical reactions of Cu(II) complexes with various organic ligands are of crucial importance for their potential uses in environmental, industrial, and biological processes.

Photochemical redox reactions involving Cu(II) have been studied for many Cu(II) complex systems, such as Cu(II)/halide, carboxylate, aminocarboxylate, and polyamine.[1,2,16,26−33] Although the ligand-to-metal charge-transfer (LMCT) irradiations induce the formation of Cu(I) and the decomposition of ligands,[34−36] only a few investigations have used incident light in the environmentally relevant wavelength range (λ > 290 nm). In a series of structurally related dicarboxylate ligand systems,[28,29] equilibrium Cu(II) speciation calculations were used to determine molar absorptivities and Cu(I) quantum yields for individual Cu(II)/dicarboxylate complexes at 313 nm.[37] Cu(I) quantum yields for these complexes were found to be affected by two factors, the relative stability of the carbon-centered radical and the degree of outer-sphere coordination.

The interaction of copper with amino acids is of interest due to their prevalence in environmental and biological systems.[38−40] Photochemical properties of Cu(II)/amino acid complexes with glycine, L-valine, L-serine, L-aspartic acid, L-glutamic acid, L-histidine, L-alanine, and β-alanine have been studied.[16,30−32] Under irradiation at 310 nm in deaerated solutions, Cu(I) quantum yields from CuL_2 were found to be 0.025, 0.063, 0.066, 0.098, and 0.001 for L = glycine, L-aspartic

Received: December 21, 2013
Published: May 8, 2014

   dx.doi.org/10.1021/ic4031238 | Inorg. Chem. 2014, 53, 4934−4943

Table 1. Composition Matrix for the Calculated Equilibrium Speciation of Cu(II): Cu(II) Species and Their Corresponding Components, Stoichiometric Coefficients, and Equilibrium Formation Constants

	components						equilib. constant[a]	
species	Cu^{2+}	CO_3^{2-}	H^+	L-alanine$^-$	PO_4^{3-}	Cl^-	$\log_{10}(\beta)$	notes[b]
Cu(L-alanine)$^+$	1			1			8.11	0.1
Cu(L-alanine)$_2^0$	1			2			14.90	0.1
$Cu(HPO_4)^0$	1		1		1		14.79	0.1
$Cu(H_2PO_4)^+$	1		2		1		18.49	3.0
$CuCl^+$	1					1	−0.14	→ 0
$Cu(Cl)_2^0$	1					2	−0.93	→ 0
$Cu(Cl)_3^-$	1					3	−2.95	→ 0
$Cu(Cl)_4^{2-}$	1					4	−5.03	→ 0
$Cu(OH)^+$	1		−1				−7.68	0.1
$Cu(OH)_2^0$	1		−2				−16.43	→ 0
$Cu(OH)_3^-$	1		−3				−26.81	1.0
$Cu(OH)_4^{2-}$	1		−4				−39.57	1.0
$Cu_2(OH)^{3+}$	2		−1				−5.38	3.0
$Cu_2(OH)_2^{2+}$	2		−2				−10.76	0.1
$Cu_3(OH)_4^{2+}$	3		−4				−21.42	0.1
$Cu(CO_3)^0$	1	1					5.88	→ 0
$Cu(CO_3)_2^{2-}$	1	2					9.32	→ 0
$Cu(HCO_3)^-$	1	1	1				11.25	→ 0

[a]All equilibrium constants reported here are for 25 °C, 1.0 atm, and ionic strength I = 0.10 M. In certain cases, equilibrium constants have been converted from a value for another ionic strength to a value for ionic strength = 0.10 M (as listed in this table), using the Davies equation. Equilibrium formation constants (β) and pK_a values are from critical reviews.[49,50] [species] = β[component 1]^i [component 2]^j [component 3]^k ..., where [ ] signifies molar concentration of the species/component; i, j, k,... are stoichiometric coefficients for the corresponding component (given in the matrix above); and β is the equilibrium formation constant of the species. Blank entries in the table are zero. The pK_a values of the species (25 °C, 1.0 atm, I = 0.10 M; original source, and as used here) are alanine (2.33, 9.71), H_2CO_3* (6.13, 9.88), where H_2CO_3* ≡ H_2CO_3(aq) + CO_2(aq), and H_3PO_4 (1.92, 6.71, 11.65). For K_w = $[H^+][OH^-]$, $\log_{10}(K_w)$ = −13.78. [b]Ionic strength (molar) of the original source of the thermodynamic data.

acid, L-glutamic acid, β-alanine, and L-histidine, respectively.[16] Transient spectra of CuL_2 for L = glycine, L-valine, L-serine, L-aspartic acid, L-glutamic acid, and β-alanine have been investigated in flash irradiations (λ > 240 nm).[30−32] Similar copper−alkyl species are proposed as intermediates. The final product analysis of Cu(I), NH_3, and HCHO in the charge-transfer excitation of Cu(II)(glycine)$_2$ solutions has been performed under deaerated conditions.[32] However, photoproducts from Cu(II) complexes with other amino acids have not been studied in detail. Besides, the previous studies used millimolar Cu(II) concentrations, which are much higher than those in natural aquatic environments or biological systems varying from μM to less than nM. To the best of our knowledge, quantum yields of photoproducts for individual Cu(II)/amino acid complexes have not been reported, nor has the effect of the Cu(II) complex stoichiometry on photoreactivity been studied.

Oxygen dissolved in water can reduce Cu(I) concentration, and $HO_2^•/O_2^{•-}$ and H_2O_2 are produced instead.[3,41,42] These oxygen species play an important role in the copper cycle as they can act either as an oxidant or as a reductant with copper. Moreover, Cu(II)/amino acid complexes can catalyze the formation of H_2O_2 from $O_2^{•-}$.[43] The presence of oxygen can significantly affect the transient transformations induced in flash irradiations of the Cu(II)/amino acid complexes. To quantitatively characterize the photoproduction of Cu(I) from Cu(II)/amino acid complexes, it is necessary to minimize the confounding effects of rapid reoxidation of Cu(I) by O_2, $O_2^{•-}$, $HO_2^•$, and H_2O_2. Hence, it is necessary to study these reactions under deaerated conditions.

In this study, we have investigated the formation of Cu(I) and the decomposition of alanine (L) as a representative amino acid by photochemical redox reactions of Cu(II)/alanine complexes over an extensive range of pH, total Cu(II) concentration, and total alanine concentration. The concentration range of Cu(II)/alanine complexes studied has been down to μM. The objective of this study is to characterize the quantum yields of photoproducts for individual Cu(II)/alanine complexes and to elucidate the effect of the Cu(II) complex stoichiometry on quantum yields. The determination of individual quantum yield is important for the quantitative evaluations of the photolysis of Cu(II)/alanine complexes in natural aquatic systems. This information is also potentially valuable for the design and synthesis of photoswitchable and photolabile metal complexes.[24,25,44−46]

EXPERIMENTAL SECTION

Speciation Calculations. Equilibrium concentrations of all chemical species in Cu(II)/alanine solutions studied were calculated using the Visual MINTEQ 3.0 program.[47,48] Equilibrium constants and pK_a values used in these calculations are from critical reviews and listed in Table 1.[49,50] Ionic strength corrections were made using the Davies equation. The use of an equilibrium speciation model to describe the Cu(II) speciation is appropriate due to the rapid water/ligand exchange reactions of Cu(II) in aqueous solution.

Materials and Solution Preparation. All chemicals were of analytical or reagent grade, or the highest purity available from several suppliers. $CuCl_2·2H_2O$ (>99.0%), CuCl (>99.0%), NaH_2PO_4 (>99.5%), acetic acid (>99%), 2-mercaptoethanol (99.0%), *o*-phthalaldehyde (>99%), boric acid (>99.8%), methanesulfonic acid (MSA) (>98%), and hydroxylammonium chloride (>99.0%) were obtained from Merck (Darmstadt, Germany). Sodium hydroxide (>98.9%), sulfuric acid (>96.0%), hydrochloric acid (36.5−38%), methanol, and acetonitrile were from J.T. Baker. Acetaldehyde (>98%), L-alanine (L-α-alanine) (>99.5%), and β-alanine (>99.5%) were obtained from Fluka (Buchs, SG, Switzerland). Ammonium

dx.doi.org/10.1021/ic4031238 | Inorg. Chem. 2014, 53, 4934−4943

chloride (>99.5%), sodium chloride (>99.8%) and sodium phosphate (>98%) were obtained from Riedel-deHaën (Seelze, Germany). 2,4-Dinitrophenylhydrazine (>97%, Sigma, St. Louis, MO, USA) was recrystallized in hexane−dichloromethane with the ratio of 7:3 (v/v) prior to use. Other reagents used were D-alanine (99%, Alfa Aesar), 2-nitrobenzaldehyde (98%, Aldrich), and bathocuproine (sulfonated sodium salt, GFS). Ultra-high-purity N_2 (99.9995%) equipped with an O_2 trap (Oxiclear DGP-250-R1, Labclear) was used to purge solutions of bathocuproine and Cu(II)/alanine. All solutions were prepared using only ultra-high-purity Milli-Q water (≥18.2 MΩ·cm resistivity). Solutions (or aliquots) were filtered through a 0.2 μm syringe filter (13 mm Teflon, or 25 mm Tuffryn; Acrodisc, Gelman). Glassware and quartzware were cleaned using a 50/50 v/v mixture of methanol and aqueous 3.0 M HCl and thoroughly rinsed with Milli-Q water.[51]

Table 2 summarizes the solution conditions used for this study, which were optimized from the equilibrium speciation calculations.

Table 2. Composition of Cu(II)−L-Alanine Solutions[a]

measurement	$[Cu(II)]_T$, μM	$[alanine]_T$, mM	pH
molar absorbance	50	0.30−1.00	6.50
	50	1.00	7.0−8.0
	50	5.00	4.75−6.00
	500	5.00−40.00	5.00
	500	50.00	3.75−5.50
	5000	20.00	4.50−6.00
Cu(I) formation	30−1000	2.00	6.00
	30	2.00	7.00
	50	0.06−5.00	6.00
	50	0.10−2.00	7.00
	50	1.00	5.50−8.00
	50	2.00	5.25−7.00
	50	2.00−20.00	5.00
ammonia formation	100−1000	2.00	5.80
	200	1.00−40.00	5.80
	200	2.00	5.50−7.50
acetaldehyde formation	50	0.3−50.00	6.00
	50	2.00	5.00−7.00
	50−1000	2.00	6.00
	200	2.00, 40.00	5.80

[a]All solutions were studied at 25 °C, contained 100 μM total orthophosphate to buffer the pH (±0.03), had an ionic strength of 0.10 M (adjusted with NaCl, almost always 0.10 M), and were filtered (0.2 μm). All solutions for photochemical experiments and Cu(I) measurements were N_2-purged. All solutions for spectral measurements were saturated with ambient laboratory air. Solutions did not contain any precipitates and were below the calculated solubility limit of all solids. $[Cu(II)]_T$ = total concentration of Cu(II). $[alanine]_T \equiv$ total concentration of alanine ligand. The exact composition of each solution studied is described in the Supporting Information.

Typically, total initial concentration of Cu(II) ($[Cu(II)]_T$) and total initial concentration of L-alanine ligand ($[L]_T$) were held constant while pH was varied, or pH and $[Cu(II)]_T$ were kept constant while $[L]_T$ was varied. In some cases, pH and $[L]_T$ were kept constant while $[Cu(II)]_T$ was varied. The criteria of a minimum absorbance of ≈0.005 (at 313 nm) due solely to Cu(II) species almost always limited the lowest total Cu(II) concentration that could be used for photochemical experiments.

Analytical Equipment and Measurements. Ultraviolet−visible absorbance measurements were made with a double-beam scanning spectrophotometer (Shimadzu UV-1601, Tokyo, Japan) and a custom-built constant-temperature (25 °C, Fisher 910 recirculator) variable-path-length aluminum cuvette holder (black-anodized). Absorbance measurements of Cu(II) solutions were carried out in Teflon-stoppered 1.00, 5.00, or 10.00 cm quartz cuvettes (Hellma, Spectrocell, or Starna). A monochromatic irradiation system (mainly from Spectral Energy Corp., Kratos, Schoeffel) was constructed from a high-pressure 1000 W O_3-free Hg−Xe lamp (ORC), a water filter (8 cm, Oriel 6214), a monochromator (entrance and exit slits = 2.5 mm; full bandwidth at half-peak-height = 7−8 nm) with holographic grating (1200 grooves/mm, Milton Roy), two 2.5 mm Hoya UV-30 optical glass filters to filter light exiting the monochromator, a shutter, and a black reaction chamber. The reaction chamber contains a black-anodized Al cuvette holder that maintains a gastight 100% fused-quartz rectangular cuvette (5.00 cm path length, Spectrocell Inc.; R-3050-I; FUV; modified to 70 mm overall height) in a tightly fixed, reproducible position at constant temperature between spring-loaded, temperature-controlled side walls, and stirs the solution with a Teflon-coated magnetic stir bar (1 mm diameter, 8 mm long). Photochemical experiments and chemical actinometry were done in the aforementioned 5.00 cm quartz cuvettes equipped with a 12 mm Teflon-faced silicone septum (Sun Brokers, 200594) and a Teflon screw cap.

Cu(I) was quantitatively determined using the bathocuproinedisulfonate method with the literature value of the Cu(I)-based molar absorptivity at 484 nm of 1.24×10^4 M^{-1} cm^{-1}.[29] N_2-purging was used to remove O_2 from solutions of Cu(II)/L-alanine, bathocuproine, Cu(I), and Cu(II) to ensure an accurate measurement of Cu(I). Ammonia was measured by a purge-and-trap ion chromatography method developed previously for the determination of trace amounts of ammonium ion in high-salinity water samples.[52,53] Aldehydes were determined by HPLC using 2,4-dinitrophenylhydrazine (DNPH) derivatization described previously.[54] The modified HPLC-DNPH method is particularly well-suited for the determination of aldehydes in heavy metal containing waters. In acidic aqueous solutions, the hydrazone derivatives could be hydrolyzed back to aldehydes and DNPH. The formation equilibrium constant was used to compensate the decrease of hydrazone derivatives.[55,56] The equilibrium constant for the formation of acetaldehyde DNP hydrazone derivative at 25 °C was 3.6×10^4 M^{-1}. Quantitative determination of amines was carried out by vortex-assisted liquid−liquid microextraction coupled with derivatization reported previously.[57] 2-Nitrobenzaldehyde (2-NB) chemical actinometry was used to determine photon fluxes at 313 nm. Photolysis of 2-NB in aqueous solution leads to the formation of 2-nitrosobenzoic acid, and the disappearance of 2-NB could be monitored using reverse-phase HPLC (Beckman Ultrasphere 5 um C-18 analytical column, 15 cm) with 40% acetonitrile in water as eluent and UV detection at 260 nm. Solution pH was measured with an Ioncheck 45 pH meter (Radiometer Analytical) and combination glass electrode (Mettler Toledo Inlab 439/120). The pH of the sample solution was adjusted by adding aliquots of 0.1 or 0.01 M NaOH to the desired pH. The pH of the buffer was checked periodically and readjusted when necessary.

Data Analysis. UV−vis absorption spectra data were analyzed with multivariate curve resolution-alternating least-squares (MCR-ALS), one of the current chemometric techniques used for the analysis of spectrophotometric data and the resolution of the different species present in multiequilibria systems.[58−60] The homemade program for the MCR-ALS algorithm was implemented in Matlab (Mathworks Inc., version R2009b). Molar absorptivities (ε_i, M^{-1} cm^{-1}) at a given wavelength for individual species reported here were determined as[37]

$$\varepsilon_{Cu(II)} = \sum_i \varepsilon_i f_i \quad (1)$$

where $\varepsilon_{Cu(II)}$ is the experimental Cu(II)-based molar absorptivity and f_i is the equilibrium fraction of the total copper present as the ith complex (e.g., $f_{CuL} \equiv [CuL]/[Cu(II)]_T$, $f_{CuL_2} \equiv [CuL_2]/[Cu(II)]_T$, $f_{in} \equiv [Cu(II)]_{in}/[Cu(II)]_T$, where f_{in} represents the fraction of all forms of inorganic Cu(II) species).

The quantum yield gives the probability of the excited molecules transformed per quantum of light absorbed. As an example, the measured total rate of Cu(I) photoproduction ($R_{Cu(I)}^0$, M s^{-1}) in the

dx.doi.org/10.1021/ic4031238 | Inorg. Chem. 2014, 53, 4934−4943

solution at a given wavelength is proportional to the absorbed light and can be expressed as

$$R_{Cu(I)}^{0} = d[Cu(I)]/dt = \Phi_{Cu(I)} I_{abs} \quad (2)$$

where I_{abs} is the fraction of the volume-averaged incident irradiance absorbed by Cu(II) species (einstein L^{-1} s^{-1}) and $\Phi_{Cu(I)}$ is the experimental average Cu(I) quantum yield (mole einstein^{-1}). When the measured total absorbance of the solution (A) is due to Cu(II) species only, $R_{Cu(I)}^{0}$ can be also expressed as[37]

$$R_{Cu(I)}^{0} = \Phi_{Cu(I)} I_0 \{1 - \exp[-\ln(10)(A)]\} \quad (3)$$

where I_0 is the volume-averaged incident irradiance (einstein L^{-1} s^{-1}). For an aqueous Cu(II) solution with low total absorbance ($A \leq 0.042$) where the Beer's law is valid and where the conversion of Cu(II) to Cu(I) is limited to <10% of the total initial Cu(II) concentration, the initial rate of Cu(I) photoproduction can be expressed as

$$R_{Cu(I)}^{0} = [\ln(10)] I_0 D \Phi_{Cu(I)} \varepsilon_{Cu(II)} [Cu(II)]_T = j_{Cu(I)} [Cu(II)]_T \quad (4)$$

where D is the optical path length (cm) and A is equal to $\varepsilon_{Cu(II)} D [Cu(II)]_T$. The apparent first-order rate constant for Cu(I) photoproduction ($j_{Cu(I)}$) at 313 nm was determined from the linear-regression slope of a plot of $\ln\{[Cu(II)]_T/([Cu(II)]_T - [Cu(I)])\}$ versus illumination time. The initial Cu(I) photoproduction rate is the sum of the initial photoreaction rates of individual Cu(II) species; thus, Cu(I) quantum yields ($\Phi_{Cu(I),i}$, mole einstein^{-1}) for individual Cu(II) species can be determined from[37]

$$\Phi_{Cu(I)} \varepsilon_{Cu(II)} = \sum_i (\Phi_{Cu(I),i} \varepsilon_i f_i) \quad (5)$$

where the quantity $\Phi_{Cu(I)} \varepsilon_{Cu(II)}$ is determined from $j_{Cu(I)}$, I_0, and D (eq 4) and the various individual Cu(I) quantum yields (mole einstein^{-1}) are $\Phi_{Cu(I),CuL}$ for CuL, $\Phi_{Cu(I),CuL_2}$ for CuL_2, and $\Phi_{Cu(I),in}$ for the average (mean) of all inorganic Cu(II) species.

Under previous conditions, the initial photoformation rates of ammonia ($R_{NH_3}^{0}$, M s^{-1}) and acetaldehyde ($R_{CH_3CHO}^{0}$, M s^{-1}) at a given wavelength exhibit the same expression forms as eq 4 after substituting NH_3 and CH_3CHO for Cu(I), respectively. Quantum yields of ammonia and acetaldehyde (Φ_{NH_3} and Φ_{CH_3CHO}) for individual Cu(II) species can be determined from

$$\Phi_{NH_3} \varepsilon_{Cu(II)} = \sum_i (\Phi_{NH_3,i} \varepsilon_i f_i) \quad (6)$$

and

$$\Phi_{CH_3CHO} \varepsilon_{Cu(II)} = \sum_i (\Phi_{CH_3CHO,i} \varepsilon_i f_i) \quad (7)$$

where Φ_{NH_3} and Φ_{CH_3CHO} are the experimental average quantum yields of ammonia and acetaldehyde (mole einstein^{-1}), respectively, and the various individual quantum yields of ammonia and acetaldehyde are $\Phi_{NH_3,CuL}$ and $\Phi_{CH_3CHO,CuL}$ for CuL and Φ_{NH_3,CuL_2} and Φ_{CH_3CHO,CuL_2} for CuL_2, respectively.

Values of the volume-averaged incident irradiance I_0 (einstein L^{-1} s^{-1}) at 313 nm were determined by 2-nitrobenzaldehyde chemical actinometry (2-NB)

$$I_0 = j_{2\text{-NB}}/([\ln(10)] \Phi_{2\text{-NB}} \varepsilon_{2\text{-NB}} D) \quad (8)$$

where the first-order rate constant $j_{2\text{-NB}}$ for actinometer loss was determined from the linear-regression slope of the plot of $\ln([2\text{-NB}]/[2\text{-NB}]_0)$ versus illumination time and a quantum yield ($\Phi_{2\text{-NB}}$) of 0.41 ± 0.02 for 2-NB photolysis in water is recommended.[61] $\Phi_{2\text{-NB}} \varepsilon_{2\text{-NB}}$ is the product of the quantum yield and the molar absorptivity for 2-NB (650 ± 33 L einstein^{-1} s^{-1} at 313 nm). Measured experimental values of I_0 at 313 nm ranged from 0.51 to 1.74 μ(einstein) L^{-1} s^{-1}, and values of $I_0 D$ ranged from 2.5 to 8.7 n(einstein) cm^{-2} s^{-1} for these experiments.

RESULTS AND DISCUSSION

Cu(II) Speciation. Alanine shows strong complexation ability with Cu(II) and is capable of forming mono- and dialanine complexes with Cu(II). For the conditions of molar absorbance measurements, the complexes CuL and CuL_2 constituted at least 85% of the total Cu(II) species ($f_{CuL} + f_{CuL_2} > 0.85$), while the total inorganic Cu(II) species represented less than 15% of the Cu(II) in this system ($f_{in} < 0.15$) for all 38 experiments. These values also held for the conditions of photochemical experiments for all (74 experiments) but four experiments, which were required to test the effect of inorganic Cu(II) species. The calculated equilibrium speciation results of all of the experimental solutions are reported in Tables S1–S4 (Supporting Information). For the conditions of this study, inorganic Cu(II) species represented a minor fraction of the total Cu(II). Moreover, inorganic Cu(II) species absorbed more weakly and photolyzed less efficiently than Cu(II)/alanine complex species studied here.

Molar Absorptivities of Individual Cu(II) Complexes. Figure 1A shows the ultraviolet–visible (UV–vis) absorption spectra for Cu(II)/alanine complexes at different pH values. Absorbance of Cu(II)/alanine complexes shows significant pH dependence in the UV region (below 350 nm) and visible region (above 450 nm). Absorption in the visible region is attributed to weak d–d transitions, which give the solution a

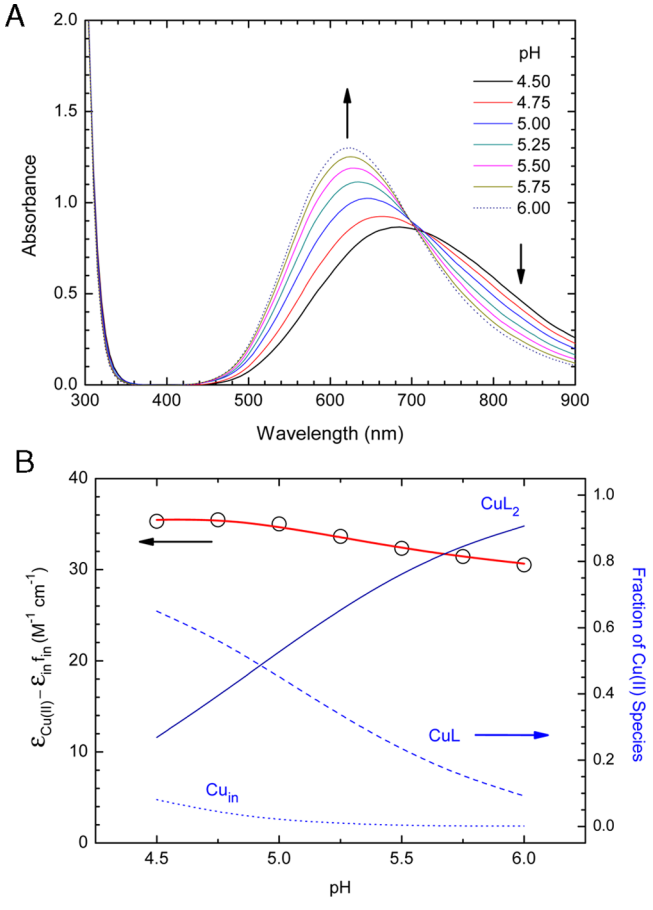

Figure 1. (A) UV–vis absorption spectra for Cu(II)/alanine complex solutions at different pH values. (B) Molar absorptivity at 313 nm and species distribution of the Cu(II)/alanine system as a function of pH. $[Cu(II)]_T$ = 5.0 mM, $[alanine]_T$ = 20.0 mM, 100 μM phosphate buffer, and 0.1 M ionic strength (NaCl).

dx.doi.org/10.1021/ic4031238 | Inorg. Chem. 2014, 53, 4934–4943

blue color but does not produce detectable photoredox reaction. Absorbance in the UV region is ascribed to LMCT, which involves the reduction of the copper and the oxidation of the ligand. UV−vis absorption spectra data were analyzed with MCR-ALS, and resolved pure spectra of two major chromophores (CuL and CuL_2) are obtained in Figure S1 (Supporting Information). Two isosbestic points were observed at 300 and 700 nm, respectively. In order to understand sunlight-initiated photochemical reactions, the molar absorptivities for individual Cu(II) complex species are characterized at wavelengths that occur in the terrestrial solar spectrum. Figure 1B shows the absorbance changes at 313 nm at various pH values. As pH increases, the molar fraction of CuL_2 increases yet the absorbance decreases, implying that the molar absorptivity of CuL_2 is lower than that of CuL at 313 nm. The best-fit curve, using two linear regression parameters, confirms the existence of two major species. To determine more precisely the molar absorptivities for individual Cu(II) complex species (CuL and CuL_2) at 313 nm, 38 absorbance measurements were made in a wide range of the solution conditions, varying in $[Cu(II)]_T$, $[L]_T$, or pH (see the Supporting Information). The relationship between the quantity $(\varepsilon_{Cu(II)} - \varepsilon_{in}f_{in})$ and the calculated equilibrium fractions of CuL (f_{CuL}) was investigated over a range of different experimental conditions.

Figure 2 illustrates the quality of fit of eq 1 where calculated values agree well with measured ones and data in Figure 1B. All

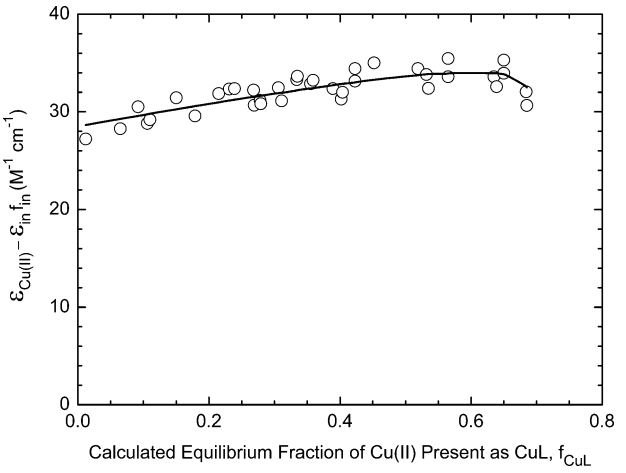

Figure 2. Comparison of measured and calculated molar absorptivities at 313 nm for 38 Cu(II)/alanine systems over a wide range of experimental conditions (see Table 2). Best-fit values were determined from eq 1.

results for the Cu(II)/alanine systems show a higher value of the molar absorptivity at 313 nm for CuL (40 M^{-1} cm^{-1}) than for CuL_2 (29 M^{-1} cm^{-1}).

Kinetics of Photoproductions from Cu(II) Complexes. As an example, Figure 3 shows the results of Cu(I) photoproduction (313 nm) for Cu(II)/alanine systems. As expected from eq 4, Cu(I) photoproduction follows first-order kinetics that is characterized by an apparent first-order rate constant for Cu(I) photoproduction ($j_{Cu(I)}$, s^{-1}, as defined in eq 4). With a similar kinetic behavior, photoproductions of NH_3 and CH_3CHO (313 nm) for Cu(II)/alanine systems are shown in Figures S2 and S3 (Supporting Information). For all of the Cu(II)/alanine systems studied, linear regression R^2 values for first-order kinetic plots of this type were ≥0.98 for all (73

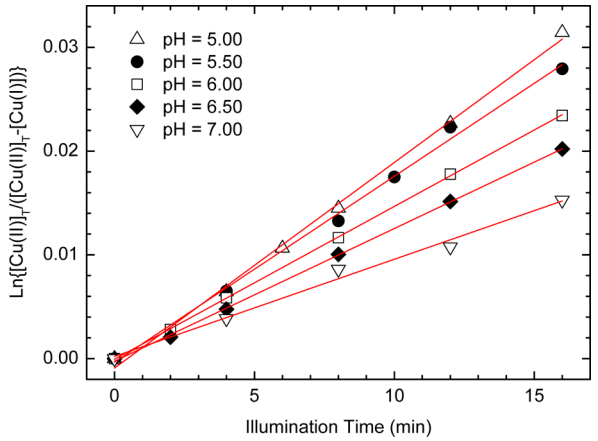

Figure 3. Kinetic behavior of Cu(I) photoproduction at 313 nm in the Cu(II)/alanine system with $[Cu(II)]_T$ = 50 μM, $[alanine]_T$ = 2.0 mM, pH = 5.00−7.00 (100 μM phosphate buffer), and 0.1 M ionic strength (NaCl). The slope of this plot gives the apparent first-order rate constant for Cu(I) photoproduction, $j_{Cu(I)}$ (eq 4).

experiments) but six experiments. Equilibrium speciation calculations for these systems (where inorganic Cu(II) species are negligible and the ligand is in large excess) indicate that the equilibrium Cu(II) speciation should not change significantly over the initial course of the reaction.

Dark control experiments show that the production rate of Cu(I), NH_3, or CH_3CHO from thermal reactions of the Cu(II)/alanine system is less than 4% of the photoformation rate. In any case, for each kinetic data point, the small concentration of Cu(I), NH_3, or CH_3CHO formed thermally was subtracted from the measured total concentration of Cu(I), ammonia, or acetaldehyde formed in the photolyzed solution. L and D forms of optical isomers for alanine were also examined on the rate of the Cu(I) photoproduction under the same experimental conditions, and no differences were observed. It indicates that L and D isomeric forms of alanine share the same reaction mechanism in the photolysis of Cu(II)/alanine complexes.

Effect of Chloride Concentration. The effect of chloride concentration on the Cu(I) photoformation rate is shown in Figure 4. The rate was found to be very sensitive to chloride concentration, increasing with the increase of chloride concentration from 0.001 to 1.0 M. This dependence is in agreement with previous studies where the oxidation rate of Cu(I) was strongly affected by chloride concentration, which could be attributed to the ability of chloride to form strong complexes with Cu(I).[62−65] The stability of Cu(I) in high NaCl solutions could not only minimize the rapid reoxidation of Cu(I) in air-saturated solutions but also increase the reduction of Cu(II) in the photolysis of Cu(II)/alanine systems studied here. Although Cu(I) photoproduction followed first-order kinetics in different chloride concentrations, the linear regression R^2 values varied from 0.859 to 0.998 and the optimum chloride concentration with the best value of R^2 occurred at 0.1 M NaCl. To quantitatively characterize the photoproduction of Cu(I) from Cu(II) complexes, 0.1 M NaCl was selected for further study where the chloride concentration would not change notably during these experiments.

Quantum Yields of Individual Cu(II) Complexes. Equation 5 indicates that the observed value, $\Phi_{Cu(I)}\varepsilon_{Cu(II)}$, is a linear combination of the weighted values of $\Phi_{Cu(I),CuL}\varepsilon_{CuL}$ and $\Phi_{Cu(I),CuL_2}\varepsilon_{CuL_2}$. Therefore, eq 5 was used to determine values of

dx.doi.org/10.1021/ic4031238 | Inorg. Chem. 2014, 53, 4934−4943

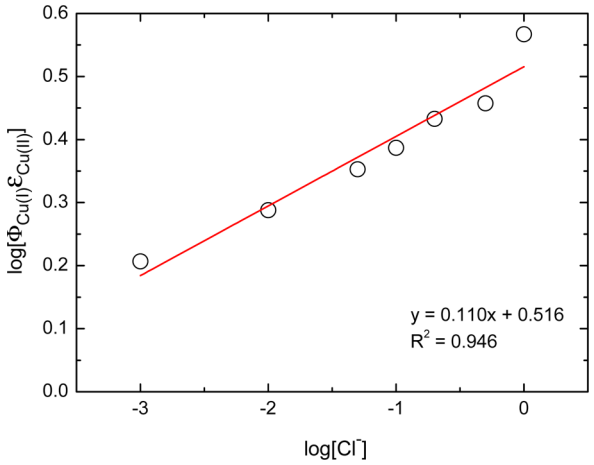

Figure 4. Effect of chloride concentration on the Cu(I) photoformation efficiency for Cu(II)/alanine complex solutions. $[Cu(II)]_T$ = 50 μM, $[alanine]_T$ = 2.0 mM, pH = 6.0, and 100 μM phosphate buffer.

$\Phi_{Cu(I),CuL}\varepsilon_{CuL}$ and $\Phi_{Cu(I),CuL_2}\varepsilon_{CuL_2}$ from which values of $\Phi_{Cu(I),CuL}$ and $\Phi_{Cu(I),CuL_2}$ were derived. As an example, Figure 5 illustrates the quality of fit of eq 5 for the Cu(II)/alanine system as a function of pH, total initial concentration of alanine ($[L]_T$), and total initial concentration of Cu(II). Each value of an apparent first-order rate constant for Cu(I) photoproduction ($j_{Cu(I)}$, s^{-1}) at a given experimental condition is shown as a single data point in Figure 5. On the basis of the regression best-fit parameters (e.g., $\Phi_{Cu(I),CuL}\varepsilon_{CuL}$ and $\Phi_{Cu(I),CuL_2}\varepsilon_{CuL_2}$) and on the independently calculated equilibrium Cu(II) speciation (e.g., f_{in}, f_{CuL}, and f_{CuL_2}), values of the quantity $\Phi_{Cu(I)}\varepsilon_{Cu(II)} - \Phi_{Cu(I),in}\varepsilon_{in}f_{in}$ were also successfully quantified by eq 5 for all 48 Cu(II)/alanine solutions. Values determined in this study were consistent within 10−20%. Since these measurements involve considerable errors in the determination of incident irradiance as well as in the analytical procedures for photoproducts, errors of the order of 10−20% are common and acceptable. These results indicate that the values of individual Cu(I) quantum yields for CuL and CuL_2 are independent of pH, $[L]_T$, and $[Cu(II)]_T$. Unlike the quenching effect of malonate in the photoformation of Fe(II) or Cu(I), free uncomplexed alanine has no apparent effect on the photoreactivity of Cu(II) complexes.[29,66,67] Similarly, quantum yields of NH_3 and CH_3CHO (Φ_{NH_3} and Φ_{CH_3CHO}) for individual Cu(II) species can be determined from eqs 6 and 7, respectively. The quality of fit for the Cu(II)/alanine system as a function of pH, $[L]_T$, and $[Cu(II)]_T$ is shown in Figures S4 and S5 (Supporting Information).

Figure 6 illustrates the relationship between the quantity $(\Phi_P\varepsilon_{Cu(II)} - \Phi_{P,in}\varepsilon_{in}f_{in})$ and the calculated equilibrium fraction of CuL (f_{CuL}) over a wide range of different experimental conditions, where P represents a photoproduct: Cu(I), NH_3, or CH_3CHO. Because of the nature of multivariate linear regression, the best-fit lines shown here are not a continuous function in two dimensions. These results indicate that variations in the photoformation efficiency of Cu(I), NH_3, and CH_3CHO in Cu(II)/alanine systems can be mainly explained based on the Cu(II) speciation. As shown in Figure 6, plots of the quantity $\Phi_P\varepsilon_{Cu(II)}$ versus f_{CuL} display a linear trend line. This could be estimated as follows. Assuming that

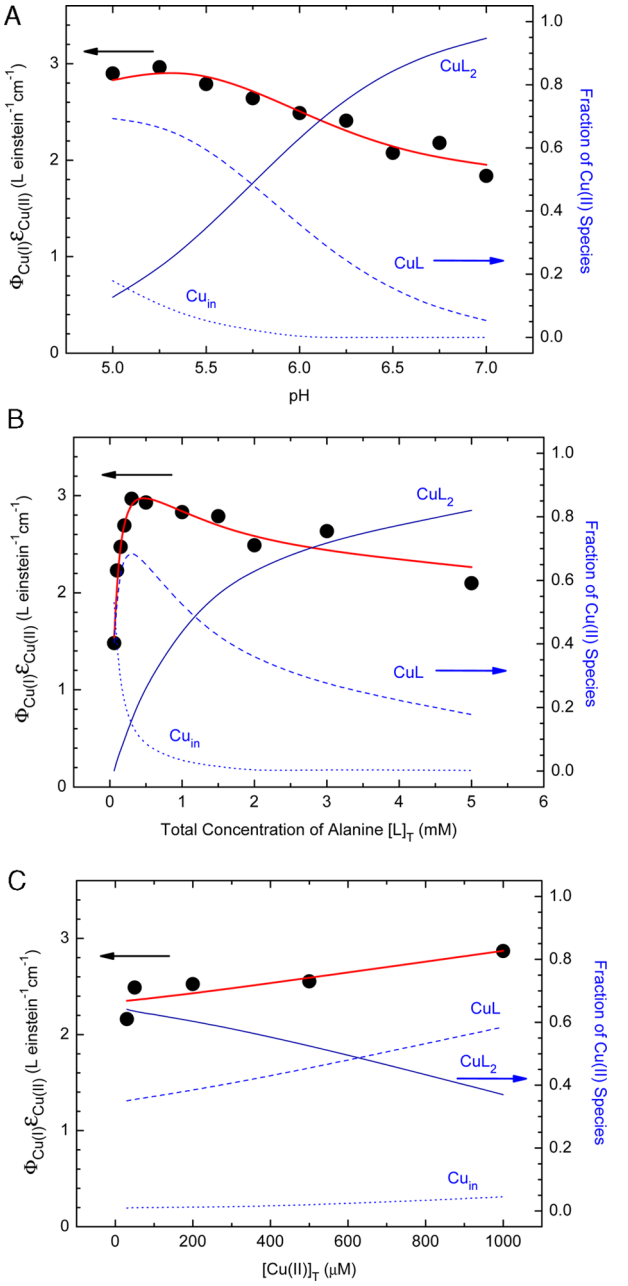

Figure 5. Comparison of measured and calculated photochemical parameters for Cu(I) photoformation and species distribution of the Cu(II)/alanine system as a function of (A) pH, (B) total concentration of alanine $[L]_T$, and (C) total concentration of Cu(II) $[Cu(II)]_T$. Best-fit values (multivariate linear regression) were determined from eq 5.

the complexes CuL and CuL_2 constitute at least 85% of the total Cu(II) species in the system, then applying $f_{CuL_2} \approx 1 - f_{CuL}$ into eq 5, 6, or 7 gives a linear equation where the slope of the line is $(\Phi_{P,CuL})(\varepsilon_{CuL}) - (\Phi_{P,CuL_2})(\varepsilon_{CuL_2})$ and the intercept is $(\Phi_{P,CuL_2})(\varepsilon_{CuL_2})$. Both the slope and the intercept exhibit the following trend for photoformation efficiency: Cu(I) > NH_3 > CH_3CHO. Values of molar absorptivities and quantum yields of Cu(I), NH_3, and CH_3CHO for the individual Cu(II) complexes are summarized in Table 3.

Cu(I) quantum yields were also determined for photolyses of the Cu(II)/alanine complexes at wavelengths of 280 and 578

dx.doi.org/10.1021/ic4031238 | Inorg. Chem. 2014, 53, 4934−4943

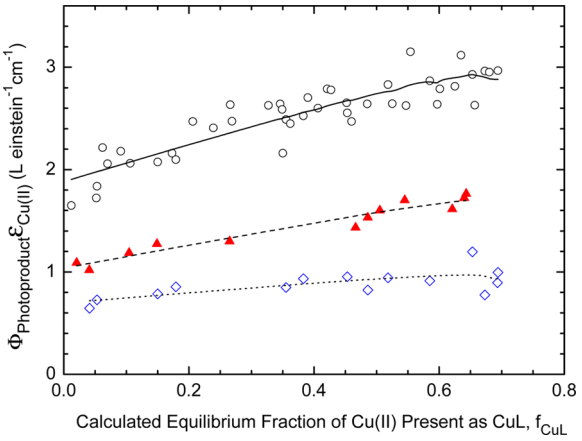

Figure 6. Comparison of measured and calculated photochemical parameters for photoproduction efficiency in the Cu(II)/alanine system as a function of the calculated equilibrium fraction of CuL (f_{CuL}) over a wide range of experimental conditions (see Table 2). Photoproduct symbols: (○) Cu(I); (▲) ammonia; (◊) acetaldehyde. Best-fit values were determined from eq 5, 6, or 7

nm. The similarity of quantum yields at 280 and 313 nm implies that the charge-transfer state is indeed reactive and that the quantum yields of Cu(I) formation are independent of the excitation wavelength in the region of the charge-transfer absorptions. In contrast, excitation at 578 nm in the d–d absorption band did not result in detectable photoreduction of Cu(II)/alanine complexes.

Proposed Mechanism and Quantum Yields of Photoproducts. The photochemical redox reactions of Cu(II)/alanine complexes produced Cu(I), NH_3, and CH_3CHO under the conditions of this study. Individual quantum yields of photoproducts listed in Table 3 vary by 4-fold from 0.094 for the Cu(I) quantum yield of CuL to 0.024 for the quantum yield of CH_3CHO of CuL_2. For both CuL and CuL_2, the individual quantum yields of Cu(I), NH_3, and CH_3CHO are in the ratio of 1.8:1:0.7. These results are in good agreement with the rates of product formation of Cu(I), NH_3, and CH_3CHO in the ratio of 2:1:1 in the charge-transfer excitation of Cu(II)(alanine)$_2$ solutions at 230 nm under deaerated conditions.[32] It was also found that the photolysis of Cu(II)(alanine)$_2$ behaved rather similarly to that of Cu(II)(glycine)$_2$, giving the final products, Cu(I), NH_3, and HCHO. The ratio of individual quantum yields of photoproducts could be explained by the oxidation of the ligand to NH_3 and CH_3CHO and reduction of an equivalent amount of Cu(II) to Cu(I). It implies that Cu(I) quantum yields include contributions from both primary photochemical processes and secondary reactions involving the carbon-centered radicals. The stability of carbon-centered radicals is expected to affect not only the Cu(I) quantum yields but also the quantum yields of NH_3 and CH_3CHO. Nevertheless, since the LMCT irradiations induce the reduction of Cu(II) to Cu(I) and the concomitant oxidation of alanine, which produces NH_3 and CH_3CHO, the quantum yields of NH_3 and CH_3CHO display a similar fashion.

On the basis of the results of this study and the literature, a plausible mechanistic pathway for the photoredox reactions of Cu(II)/alanine complexes for the 1:1 complex (CuL) is depicted in Figure 7.[16,28−33,68−70] A comparable mechanism

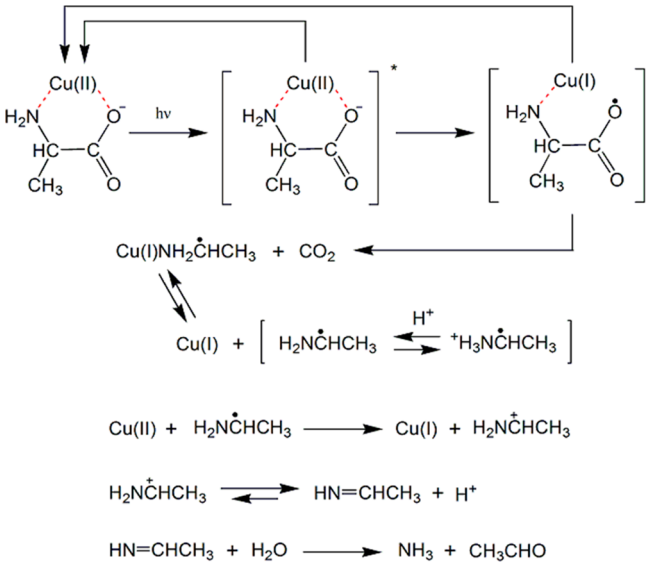

Figure 7. Proposed reaction scheme for the photoreaction of Cu(II)/alanine complexes.

would apply to the 1:2 complex (CuL_2). The irradiation of the LMCT absorption band of the Cu(II) complex initiates the primary photochemical processes that lead to an electronically excited state. The excited state undergoes two major competing reactions: it can return to the ground state by one or more mechanisms or transfer one electron from a carboxylate-centered orbital to a Cu(II)-centered orbital. The ligand radical within the water solvent cage with Cu(I) can undergo two competing reactions: it can decarboxylate, giving CO_2 and a Cu(I)/carbon-centered radical pair, or receive back the electron from Cu(I) to reform the parent Cu(II) complex. Since

Table 3. Summary of Molar Absorptivities (ε_{CuL} and ε_{CuL_2}, M^{-1} cm^{-1}) and Quantum Yields of Cu(I), Ammonia, and Acetaldehyde ($\Phi_{Cu(I),CuL}$ and $\Phi_{Cu(I),CuL_2}$, mole einstein^{-1}) for the Individual Cu(II) Complexes [Cu(alanine)$^+$(CuL) and Cu(alanine)$_2$(CuL_2)], at 313 and 280 nm[a]

photoproduct	ε_{CuL}	ε_{CuL_2}	$\Phi_{P,CuL}$	Φ_{P,CuL_2}	$(\Phi_{P,CuL})(\varepsilon_{CuL})$	$(\Phi_{P,CuL_2})(\varepsilon_{CuL_2})$	$\Phi_{P,CuL}/\Phi_{P,CuL_2}$
photolysis at 313 nm	40 ± 4	29 ± 2					
Cu(I)			0.094 ± 0.014	0.064 ± 0.012	3.74 ± 0.43	1.87 ± 0.32	1.5
ammonia			0.055 ± 0.007	0.036 ± 0.005	2.18 ± 0.18	1.04 ± 0.12	1.5
acetaldehyde			0.030 ± 0.007	0.024 ± 0.007	1.20 ± 0.25	0.70 ± 0.20	1.2
photolysis at 280 nm	500 ± 21	779 ± 15					
Cu(I)			0.094 ± 0.011	0.087 ± 0.005	46.8 ± 5.3	67.8 ± 3.3	1.1

[a]Best value ±1 standard deviation for 25 °C and 0.10 M ionic strength (NaCl). Solutions were purged with ultra-high-purity N_2 for the quantum yield determinations. The range of solution compositions used to determine these values is given in Table 2 and in the Supporting Information.

dx.doi.org/10.1021/ic4031238 | Inorg. Chem. 2014, 53, 4934−4943

carboxylate-to-Cu(II) charge-transfer states are placed at lower energies than the amino-to-Cu(II) charge-transfer states, decarboxylation rapidly follows an efficient LMCT process.[1,30] The efficiency of the back electron transfer affects the Cu(I) quantum yield. With the existence of an amino group, an efficient depopulation of the photoactive state retards the decomposition of the carboxylate radical, so the electron on the reduced Cu(I) center may be more likely to transfer back to the carboxylate radical, resulting in a low reactivity or low quantum yield of Cu(I) production. This could explain why the Cu(I) quantum yield at 313 nm for Cu(II)(alanine) is smaller than those for Cu(II)(dicarboxylate) with oxalate, malonate, or succinate.[28,29]

Although the carbon-centered radical can undergo two competing reactions, oxidation of the carbon-centered radical by bulky Cu(II) complexes, such as Cu^{2+}, CuL, and CuL_2, is favored by the dissimilar ratio of Cu(II) to Cu(I) concentrations. In contrast, the photolysis of Cu(II)(β-alanine)$_2$ under monochromatic radiation at 230 or 313 nm led to an ethylamine ($CH_3CH_2NH_2$) product and neither NH_3 nor CH_3CHO was detected.[32,57] By comparison, the photoproducts from Cu(II)/α-alanine (or L-α-alanine) and Cu(II)/β-alanine can be interpreted in terms of the reactions

$$\text{Cu(II)}/\alpha\text{-alanine} + h\nu \rightarrow \text{Cu(I)} + CO_2 + NH_3 + CH_3CHO \quad (9)$$

$$\text{Cu(II)}/\beta\text{-alanine} + h\nu \rightarrow \text{Cu(I)} + CO_2 + CH_3CH_2NH_2 \quad (10)$$

The difference in photoproducts probably reflects the distinctive structures of Cu(II) complexes with a five-membered chelate ring for α-alanine and a six-membered chelate ring for β-alanine.[71] Different carbon-centered radicals derived from decarboxylation have different degrees of stability and form different photoproducts.

Effect of Stoichiometry of Cu(II) Complexes on Photoreactivity. As can be seen from Table 3, the ratios of $\Phi_{P,CuL}$ to Φ_{P,CuL_2} are estimated to be 1.5 for Cu(I), 1.5 for NH_3, and 1.2 for CH_3CHO. The quantum yields for the 1:1 complex (CuL) are always larger than those for the 1:2 complex (CuL_2). These results are crucial because it implies that the photoreactivities of Cu(II)/amino acid complexes are underestimated when the evaluations are based on previous studies where CuL_2 is the major species. Generally, CuL is a dominant species in natural aquatic environments or biological systems where typical concentrations of Cu(II) complexes vary from μM to less than nM.

A similar effect of multiple ligands has been reported in other systems.[1,41,72−77] Kinetics of the reduction of neptunium(VI) by dicarboxylic acids show that the $NpO_2L_2^{2-}$ complex is much less labile in redox reactions than NpO_2L (L^{2-} = dicarboxylate ligand).[72] The photoreactivity of the chlorocuprate(II) complexes changes with the number of the coordinated ligands.[1] Individual quantum yields for photoreduction of chlorocuprate(II) complexes in acetonitrile at 313 nm were determined to be 0.16 for $CuCl^+$, 0.098 for $CuCl_2$, 0.028 for $CuCl_3^-$, and 0.0089 for $CuCl_4^{2-}$. The complexes containing a higher number of Cl^- ligands proved to be less efficient. A similar trend is also reported for the quantum yields of Fe(II) formation from Fe(III)−oxalato complexes.[73−75] The photoreactivity of Fe(III)−hydroxy species decreases as the mean number of bonds that must be broken to release each Fe(II) increases.[41,76,77]

A plausible explanation for this phenomenon relates to the stabilizing effect of the second ligand molecule on the copper center. The ligands studied presumably exhibit a strong preference for binding to Cu(II) rather than to Cu(I). Thus, the presence of the second ligand molecule could lower the probability of ligand-to-Cu(II) charge (electron) transfer in CuL_2 relative to that in CuL because the second ligand stabilizes copper in the II oxidation state. This Cu(II)-stabilizing effect opposes the driving force to reduce Cu(II) to Cu(I) and hence lowers the Cu(I) quantum yield for CuL_2 relative to CuL. Also, delocalizing the LMCT excitation over two carboxylate groups may stabilize the linkage and reduce chances for elimination of carbon dioxide as well.

CONCLUSIONS

In this study, molar absorptivities and quantum yields of photoproducts for Cu(II)/alanine complexes have been measured over an extensive range of experimental conditions. Individual quantum yields of Cu(I), ammonia, and acetaldehyde are determined and characterized mainly with the equilibrium Cu(II) speciation where the presence of CuL and CuL_2 is taken into account. The ratio of individual quantum yields of photoproducts could be explained by the oxidation of the ligand to NH_3 and CH_3CHO and reduction of an equivalent amount of Cu(II) to Cu(I) where both direct and indirect photochemical reactions contribute to the Cu(I) quantum yield. No differences were observed in the photolysis of Cu(II) complexes with L or D forms of alanine. Visible excitation into the d−d bands was ineffective at inducing decomposition. In view of the Cu(II)-complex stoichiometry, CuL always has larger quantum yields than CuL_2, which implies that the photoreactivities of Cu(II)/amino acid complexes could be underestimated in natural aquatic systems.

ASSOCIATED CONTENT

Supporting Information

Listings of tables and figures containing additional information about the molar absorptivities and quantum yields of photoproducts for Cu(II)/alanine complexes studied here. This material is available free of charge via the Internet at http://pubs.acs.org.

AUTHOR INFORMATION

Corresponding Author

*Tel: 886-3-5715131, ext. 35856. Fax: 886-3-5718649. E-mail: chwu@mx.nthu.edu.tw.

Notes

The authors declare no competing financial interest.

ACKNOWLEDGMENTS

We would like to thank the editor and three anonymous reviewers for their valuable comments. This work was supported by the Ministry of Science and Technology of the Republic of China (Taiwan) under Grant Numbers NSC 90-2113-M-007-025, NSC 91-2113-M-007-013, NSC 92-2113-M-007-063, NSC 98-2113-M-007-015, and NSC 100-2113-M-007-004.

REFERENCES

(1) Horvath, O.; Stevenson, K. L. *Charge Transfer Photochemistry of Coordination Compounds*; VCH: New York, 1993; pp 35−70.
(2) Sykora, J. *Coord. Chem. Rev.* **1997**, *159*, 95−108.
(3) Ciesla, P.; Kocot, P.; Mytych, P.; Stasicka, Z. *J. Mol. Catal. A: Chem.* **2004**, *224*, 17−33.
(4) Armaroli, N.; Accorsi, G.; Cardinali, F.; Listorti, A. *Top. Curr. Chem.* **2007**, *280*, 69−115.
(5) Sakamoto, R.; Kusaka, S.; Hayashi, M.; Nishikawa, M.; Nishihara, H. *Molecules* **2013**, *18*, 4090−4119.
(6) Szacilowski, K.; Macyk, W.; Drzewiecka-Matuszek, A.; Brindell, M.; Stochel, G. *Chem. Rev.* **2005**, *105*, 2647−2694.
(7) Jiang, Q.; Xiao, N.; Shi, P.; Zhu, Y.; Guo, Z. *Coord. Chem. Rev.* **2007**, *251*, 1951−1972.
(8) Pitie, M.; Pratviel, G. *Chem. Rev.* **2010**, *110*, 1018−1059.
(9) Kogut, M. B.; Voelker, B. M. *Environ. Sci. Technol.* **2003**, *37*, 509−518.
(10) Hsu-Kim, H. *Environ. Sci. Technol.* **2007**, *41*, 2338−2342.
(11) Vilar, V. J. P.; Botelho, C. M. S.; Boaventura, R. A. R. In *Security of Industrial Water Supply and Management*; Atimtay, A. T., Sikdar, S. K., Eds.; Springer: Dordrecht, The Netherlands, 2011; pp 159−173.
(12) Clara, M.; Windhofer, G.; Weilgony, P.; Gans, O.; Denner, M.; Chovanec, A.; Zessner, M. *Chemosphere* **2012**, *87*, 1265−1272.
(13) Kieber, R. J.; Skrabal, S. A.; Smith, C.; Willey, J. D. *Environ. Sci. Technol.* **2004**, *38*, 3587−3594.
(14) Buerge-Weirich, D.; Sulzberger, B. *Environ. Sci. Technol.* **2004**, *38*, 1843−1848.
(15) Witt, M. L. I.; Skrabal, S.; Kieber, R.; Willey, J. *J. Atmos. Chem.* **2007**, *58*, 89−109.
(16) Hayase, K.; Zepp, R. G. *Environ. Sci. Technol.* **1991**, *25*, 1273−1279.
(17) Andrianirinaharivelo, S. L.; Bolte, M. *J. Photochem. Photobiol., A* **1993**, *73*, 213−216.
(18) Mailhot, G.; Andrianirinaharivelo, S. L.; Bolte, M. *J. Photochem. Photobiol., A* **1995**, *87*, 31−36.
(19) Andrianirinaharivelo, S.; Mailhot, G.; Bolte, M. *Sol. Energy Mater. Sol. Cells* **1995**, *38*, 459−474.
(20) Yang, J. K.; Davis, A. P. *Environ. Sci. Technol.* **2000**, *34*, 3789−3795.
(21) Repicka, Z.; Izakovic, M.; Mazur, M.; Sima, J.; Valigura, D. *Acta Chim. Slov.* **2010**, *3*, 30−37.
(22) Szacilowski, K.; Macyk, W.; Stochel, G.; Stasicka, Z.; Sostero, S.; Traverso, O. *Coord. Chem. Rev.* **2000**, *208*, 277−297.
(23) Campanella, L.; Battilotti, M.; Lecce, R. *Int. J. Environ. Health* **2007**, *1*, 98−119.
(24) Ciesienski, K. L.; Haas, K. L.; Dickens, M. G.; Tesema, Y. T.; Franz, K. J. *J. Am. Chem. Soc.* **2008**, *130*, 12246−12247.
(25) Ciesienski, K. L.; Haas, K. L.; Franz, K. J. *Dalton Trans.* **2010**, *39*, 9538−9546.
(26) Das, S.; Johnson, G. R. A. *J. Chem. Soc., Faraday Trans. 1* **1980**, *76*, 1779−1789.
(27) Glebov, E. M.; Plyusnin, V. F.; Grivin, V. P.; Krupoder, S. A.; Liskovskaya, T. I.; Danilovich, V. S. *J. Photochem. Photobiol., A* **2000**, *133*, 177−183.
(28) Sun, L.; Wu, C.-H.; Faust, B. C. *J. Phys. Chem. A* **1998**, *102*, 8664−8672.
(29) Wu, C.-H.; Sun, L.; Faust, B. C. *J. Phys. Chem. A* **2000**, *104*, 4989−4996.
(30) Natarajan, P.; Ferraudi, G. *Inorg. Chem.* **1981**, *20*, 3708−3712.
(31) Namasivayam, C.; Natarajan, P. *J. Polym. Sci., Polym. Chem. Ed.* **1983**, *21*, 1371−1384.
(32) Das, S.; Johnson, G. R. A.; Nazhat, N. B.; Saadalla-Nazhat, R. *J. Chem. Soc., Faraday Trans. 1* **1984**, *80*, 2759−2766.
(33) Natarajan, E.; Ramamurthy, P.; Natarajan, P. *Proc. Indian Acad. Sci., Chem. Sci.* **1990**, *102*, 319−328.
(34) Rorabacher, D. B. *Chem. Rev.* **2004**, *104*, 651−697.
(35) Holm-Jorgensen, J. R.; Jensen, M.; Bjerrum, M. J. *Inorg. Chem.* **2011**, *50*, 12705−12713.
(36) Torres, S.; Ferraudi, G.; Aguirre, M. J.; Isaacs, M.; Matsuhiro, B.; Chandia, N. P.; Mendoza, L. *Helv. Chim. Acta* **2011**, *94*, 293−300.
(37) Faust, B. C. *Environ. Sci. Technol.* **1996**, *30*, 1919−1922.
(38) Rode, B. M.; Suwannachot, Y. *Coord. Chem. Rev.* **1999**, *190−192*, 1085−1099.
(39) Yamauchi, O.; Odani, A.; Takani, M. *J. Chem. Soc., Dalton Trans.* **2002**, 3411−3421.
(40) Shimazaki, Y.; Takani, M.; Yamauchi, O. *Dalton Trans.* **2009**, 7854−7869.
(41) Faust, B. C. In *Aquatic and Surface Photochemistry*; Helz, G. R., Zepp, R. G., Crosby, D. G., Eds.; CRC Press: Boca Raton, FL, 1994; pp 3−37.
(42) Faust, B. C. In *Environmental Photochemistry*; Boule, P., Ed.; Springer: Berlin, Germany, 1999; pp 101−122.
(43) Cabelli, D. E.; Bielski, B. H. J.; Holcman, J. *J. Am. Chem. Soc.* **1987**, *109*, 3665−3669.
(44) Sasaki, Y.; Iwamoto, S.; Mukai, M.; Kikuchi, J. *J. Photochem. Photobiol., A* **2006**, *183*, 309−314.
(45) Ordronneau, L.; Nitadori, H.; Ledoux, I.; Singh, A.; Williams, J. A. G.; Akita, M.; Guerchais, V.; Bozec, H. L. *Inorg. Chem.* **2012**, *51*, 5627−5636.
(46) Marchi, E.; Baroncini, M.; Bergamini, G.; van Heyst, J.; Vogtle, F.; Ceroni, P. *J. Am. Chem. Soc.* **2012**, *134*, 15277−15280.
(47) Gustafsson, J. P. *MINTEQA2 version 4.0* and *Visual MINTEQ version 3.0*; Department of Land and Water Resources Engineering, Royal Institute of Technology (KTH): Stockholm, Sweden, 2012.
(48) Allison, J. D.; Brown, D. S.; Novo-Gradac, K. J. *MINTEQA2/PRODEFA2, A Geochemical Assessment Model for Environmental Systems*, Version 4.0; EPA/600/3-91/021; U. S. Environmental Protection Agency: Athens, GA, 1999.
(49) Smith, R. M.; Martell, A. E. *Critical Stability Constants*; Plenum: New York, 1976−1989: Vols. *1*−*6*.
(50) Martell, A. E.; Smith, R. M.; Motekaitis, R. J. *NIST Standard Reference Database 46: NIST Critically Selected Stability Constants of Metal Complexes*, Version 7.0; NIST: Gaithersburg, MD, 2003.
(51) Lin, T. Y.; Wu, C. H. *J. Catal.* **2005**, *232*, 117−126.
(52) Wang, P. Y.; Wu, J. Y.; Chen, H. J.; Lin, T. Y.; Wu, C. H. *J. Chromatogr. A* **2008**, *1188*, 69−74.
(53) Lin, T. Y.; Pan, Y. T.; Lee, H. Y.; Wang, P. Y.; Wu, C. H. *J. Chin. Chem. Soc.* **2012**, *59*, 718−726.
(54) Lin, Y. L.; Wang, P. Y.; Hsieh, L. L.; Ku, K. H.; Yeh, Y. T.; Wu, C. H. *J. Chromatogr. A* **2009**, *1216*, 6377−6381.
(55) Uchiyama, S.; Kaneko, T.; Tokunaga, H.; Ando, M.; Otsubo, Y. *Anal. Chim. Acta* **2007**, *605*, 198−204.
(56) Zhou, X.; Huang, G.; Civerolo, K.; Schwab, J. *Environ. Sci. Technol.* **2009**, *43*, 2753−2759.
(57) Chang, W. Y.; Wang, C. Y.; Jan, J. L.; Lo, Y. S.; Wu, C. H. *J. Chromatogr. A* **2012**, *1248*, 41−47.
(58) Rodriguez-Rodriguez, C.; Amigo, J. M.; Coello, J.; Maspoch, S. *J. Chem. Educ.* **2007**, *84*, 1190−1192.
(59) Cavanillas, S.; Alberich, A.; Serrano, N.; Diaz-Cruz, J. M.; Arino, C.; Esteban, M. *Analyst* **2012**, *137*, 5420−5427.
(60) De Luca, M.; Ioele, G.; Mas, S.; Tauler, R.; Ragno, G. *Analyst* **2012**, *137*, 5428−5435.
(61) Galbavy, E. S.; Ram, K.; Anastasio, C. *J. Photochem. Photobiol., A* **2010**, *209*, 186−192.
(62) Millero, F. J. *Physical Chemistry of Natural Waters*; Wiley: New York, 2001; pp 515−581.
(63) Gonzalez-Davila, M.; Santana-Casiano, J. M.; Gonzalez, A. G.; Perez, N.; Millero, F. J. *Marine Chem.* **2009**, *115*, 118−124.
(64) Pham, A. N.; Rose, A. L.; Waite, T. D. *J. Phys. Chem. A* **2012**, *116*, 6590−6599.
(65) Yuan, X.; Pham, A. N.; Xing, G.; Rose, A. L.; Waite, T. D. *Environ. Sci. Technol.* **2012**, *46*, 1527−1535.
(66) Wang, Z.; Chen, X.; Ji, H.; Ma, W.; Chen, C.; Zhao, J. *Environ. Sci. Technol.* **2010**, *44*, 263−268.
(67) Weller, C.; Horn, S.; Herrmann, H. *J. Photochem. Photobiol., A* **2013**, *268*, 24−36.

(68) Karpel Vel Leitner, N.; Berger, P.; Legube, B. *Environ. Sci. Technol.* **2002**, *36*, 3083−3089.
(69) Goldstein, S.; Czapski, G.; Cohen, H.; Meyerstein, D. *Inorg. Chem.* **1992**, *31*, 2439−2444.
(70) Matsushita, M.; Tran, T. H.; Nosaka, A. T.; Nosaka, Y. *Catal. Today* **2007**, *120*, 240−244.
(71) Martell, A. E.; Hancock, R. D. *Metal Complexes in Aqueous Solutions*; Plenum: New York, 1996.
(72) Rao, L. F.; Choppin, G. R. *Inorg. Chem.* **1984**, *23*, 2351−2354.
(73) Zuo, Y.; Hoigne, J. *Environ. Sci. Technol.* **1992**, *26*, 1014−1022.
(74) Faust, B. C.; Zepp, R. G. *Environ. Sci. Technol.* **1993**, *27*, 2517−2522.
(75) Weller, C.; Horn, S.; Herrmann, H. *J. Photochem. Photobiol., A* **2013**, *255*, 41−49.
(76) Lee, C.; Yoon, J. *Chemosphere* **2004**, *57*, 1449−1458.
(77) Arakaki, T.; Saito, K.; Okada, K.; Nakajima, H.; Hitomi, Y. *Chemosphere* **2010**, *78*, 1023−1027.